

Optical Nonlinearity and Photoinduced Anisotropy of an Azobenzene-Containing Ionic Liquid Crystalline Polymer

Fuli Zhao, Changshun Wang, Yi Zeng, Jinwen Zhang

Department of Physics, State Key Laboratory of Advanced Optical Communication Systems and Networks, Shanghai Jiao Tong University, Shanghai, People's Republic of China

Correspondence to: C. Wang (E-mail: cswang@sjtu.edu.cn)

ABSTRACT: The nonlinear optical properties of an azobenzene-containing ionic liquid crystalline polymer were investigated using single-beam Z-scan and optical Kerr effect (OKE). The polymer film exhibited large nonlinear absorption ($\sim 10^{-6}$ cm W $^{-1}$) and nonlinear refraction ($\sim 10^{-11}$ cm 2 W $^{-1}$) under 532 nm ps excitation. The femtosecond time-resolved OKE results suggested that the nonlinear optical response time in off-resonant region was as fast as 300 fs. Moreover, stable molecular reorientation and a large photoinduced birefringence ($\sim 10^{-1}$) were achieved in the polymer film with a 405 nm continuous wave (CW) laser as pump light. The large optical nonlinearity, ultrafast response, and effective photoinduced molecular reorientation of the polymer films indicated their potential applications in nonlinear photonic devices and optical storage. © 2013 Wiley Periodicals, Inc. *J. Appl. Polym. Sci.* 130: 406–410, 2013

KEYWORDS: optical properties; properties; characterization; films

Received 9 October 2012; accepted 22 January 2013; published online 18 March 2013

DOI: 10.1002/app.39097

INTRODUCTION

Over the past few decades, intensive research has been carried out for the development of versatile materials with large optical nonlinearities and high photosensitivity because of their potential applications such as all-optical switching, optical storage, and nonlinear optical devices.^{1–3} Photoresponsive polymers containing azobenzene chromophores, as a promising candidate, have intrigued considerable interest for their large nonlinear refraction and photoinduced anisotropy.^{4,5} Azobenzene groups display trans to cis transformation under actinic irradiation and reorientation in the direction perpendicular to the polarization of pump light. The anisotropic orientation of the azobenzene groups leads to in-plane birefringence, which can be nondestructively read with a nonresonant probe beam. When combined with liquid crystal (LC) character, optical control can be further enhanced by exploiting the inherent anisotropy of LC materials.^{6–8} Recently, investigations are mostly focused on the ionic self-organized supramolecular materials consisting of azobenzene photosensitive units.^{9–11} These materials combine rigidity, liquid crystallinity, and ionic polymer properties, which open wide possibilities for optical applications. Moreover, photoinduced isomerization of azobenzene molecules makes it easy to modify linear and nonlinear polarizabilities of molecular as well as optical nonlinear refraction.^{12,13} Based on the significant physicochemical properties

of these supramolecular materials, we could expect them to be good candidates for high-density optical storage and fabricating nonlinear optical devices.

In this work, we presented the results of our studies on the nonlinear response and photoinduced anisotropy of a newly synthesized azobenzene-containing ionic liquid crystalline polymer. By carrying out traditional Z-scan measurement, large third-order nonlinear refractive index was obtained in thin film under the excitation of 38 ps laser pulses at 532 nm. Under off-resonant excitation, ultrafast response was observed by using femtosecond optical Kerr effect (OKE) technique at 800 nm. Stable photoinduced molecular reorientation and large photoinduced birefringence with the value in order of 10^{-1} were obtained at low fluences.

EXPERIMENTAL

Material and Film Preparation

The sample is prepared through self-assembly. A 5 mg mL $^{-1}$ sodium polyacrylate (PANA) aqueous solution, obtained from the neutralization of polyacrylate with sodium hydroxide, was added dropwise to NDAZO (3-(6-(4-((4-(dimethylamino)phenyl)diazanyl)phenoxy)hexyl)-1-methyl-1H-imidazol-3-ium bromide) aqueous solution with the concentration of 1 mg mL $^{-1}$, i.e., in a 1 : 1 molar charge ratio. The resulting precipitated was collected by filtration and washed thoroughly with deionized water to

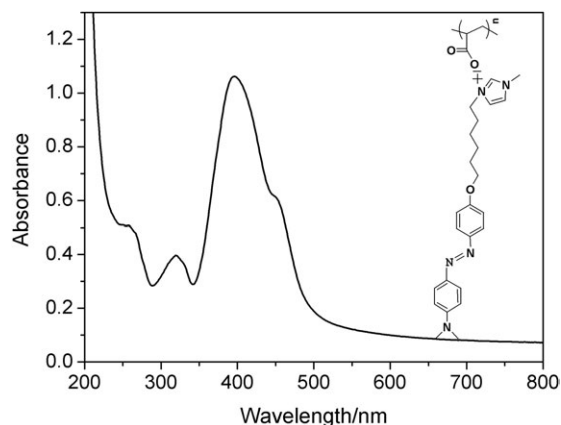


Figure 1. UV-vis absorption spectrum of the polymer film. The molecular structure of the polymer is shown in the inset.

remove residual salts and possible noncomplexed precursors and then dried in vacuum at 60°C for 24 h. Thin films of the synthesized polymer were prepared by spin-coating chloroform solution (concentration: 30 mg mL⁻¹) onto the glass slides (speed: 2000 rpm, time: 20 s). The thickness of the resultant films was about 300 nm, measured by a Dektak profilometer. Figure 1 shows the molecular structure and the UV-vis absorption spectra of the polymer. The maximum absorbance in thin film is at the wavelength of 395 nm.

Measurement of the Third-Order Optical Nonlinearities

The nonlinear optical measurements were performed using the single-beam *Z*-scan technique, which is a simple and sensitive method to determine the nonlinear refraction index and nonlinear absorption coefficient. The experimental setup in our experiment was similar to that reported in Ref. 14. In this experiment, the excitation source was a mode-locked Nd:YAG laser with 38 ps pulse duration at 532 nm. The repetition frequency was 10 Hz, and the detector was a dual-channel energy meter (EPM2000). The Gaussian laser beam was focused on the sample by a lens of 30 cm length focus, and the spot size at focal point was measured to be 29.3 μm. Before dealing with the sample, the *Z*-scan experiment on CS₂ with the thickness of 1 mm was first done for testing and calibration. Through measurement and calculation, the third-order nonlinear refractive index of CS₂ was equal to 2.76 × 10⁻¹⁸ m² W⁻¹, namely, 1.07 × 10⁻¹¹ esu, which was in good agreement with 1.2 ± 0.2 × 10⁻¹¹ esu reported previously.¹⁴

To determine the nonlinear optical response of the polymer film, a standard femtosecond OKE experiment was performed. The femtosecond laser pulse was generated from a mode-locked Ti:Sapphire oscillator (Mai Tai HP-1020) generating 100 fs pulses at 800 nm. A regenerative amplifier system (Spectra-Physics, Spitfire Pro) was used to amplify the pulses 10⁶ times at a repetition rate of 1 kHz. The beam was split into two parts with intensity ratio of 10 : 1, and the polarization of the probe beam was adjusted by 45° to the pump. The two beams were focused by a 50 cm focal length lens and overlapped on the same spot of the sample with a spot size of 200 μm. The generated OKE signal was detected by a silicon photodiode connected to a lock-in amplifier.

Measurement of the Photoinduced Anisotropy

For the measurement of photoinduced dichroism, a P-polarized (α = 0°) CW 405 nm laser beam was employed as the pump light. The polarized absorption spectra with the maximum absorbance at λ = 395 nm were measured using a Perkin-Elmer lambda 750 UV-vis spectrophotometer equipped with a step-motor-controlled Glan-Taylor prism. The in-plane order parameter, *S*, was evaluated by¹⁵:

$$S = \frac{A_{\perp} - A_{\parallel}}{A_{\perp} + 2A_{\parallel}} \quad (1)$$

where *A*_⊥ and *A*_∥ are the absorbance perpendicular and parallel to the polarization of the pump light, respectively.

A standard experimental setup was employed for the measurement of the photoinduced birefringence.¹⁶ A continuous 405 nm laser beam was employed as the pump light, and a 650 nm diode laser beam which was outside the absorption band of the sample was employed as the probe light. The polymer film was placed between two crossed polarizers in the path of the probe light, and the pump light was set to linearly polarized at ±45° with respect to the polarizers. The real-time behavior of photoinduced birefringence was measured with the photo-detector and lock-in amplifier. The birefringence value can be obtained by

$$I_T = I_0 \sin^2(\pi \Delta n d / \lambda), \quad (2)$$

where Δ_{*n*} is the photoinduced birefringence, *I*_{*T*} is the probe intensity passing through the crossed polarizers, *I*₀ is the probe intensity passing through the parallel polarizers before pump irradiation, and *d* is the thickness of thin film.

RESULTS AND DISCUSSION

In *Z*-scan experiments, the nonlinear absorption of sample was calculated using the open aperture (OA) *Z*-scan technique. If there is nonlinear absorption existing in the film, the closed transmittance is affected by the nonlinear refraction and nonlinear absorption, and it is necessary to separate the effect of nonlinear absorption. Figure 2 shows the *Z*-scan experimental data for OA curve and closed aperture (CA) curve divided by OA curve (CA/OA) of the polymer thin film under 38 ps pulse 532 nm excitation. The OA (open circles) curve displayed in Figure 2 is symmetric with respect to the focus (*z* = 0), where it has a maximum transmission. The solid line is theoretical fit according to eq. (3). The normalized transmittance for OA *Z*-scan experiment is given by

$$T(z, s = 1) = \sum [-q_0(z, 0)]^m / (m + 1)^{3/2}, \quad (q_0(0) < 1), \quad (3)$$

where *q*₀(*z*, 0) = β*I*₀*L*_{eff} / (1 + *z*²/*z*₀²), *z*₀ = *kω*₀²/2 is the diffraction length of the beam, and ω₀ is the beam waist radius at the focus point. *L*_{eff} = (1 - exp(-α*L*))/α is the effective thickness of the sample, α is the linear absorption coefficient, and *L* is the thickness of the sample.¹⁴ The value of confocal parameter *z*₀ at the focus was calculated to be 5.06 mm, much longer than the thickness of the thin film. The laser intensity at the focus was calculated to be 5.88 GW cm⁻². The linear absorption coefficient

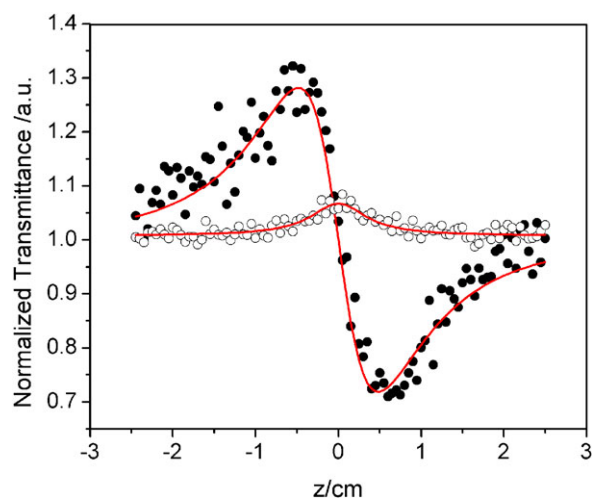


Figure 2. Examples of Z-scan measured at $I_0 = 5.88 \text{ GW cm}^{-2}$ for the 300-nm-thick polymer film under 38 ps 532 nm excitation. Open and filled circles are the OA and CA/OA Z-scan data, respectively, and the solid lines are the best-fit curves calculated by Z-scan theory. [Color figure can be viewed in the online issue, which is available at wileyonlinelibrary.com.]

was $\alpha = 1.03 \times 10^4 \text{ cm}^{-1}$, and the effective thickness of the sample was $L_{\text{eff}} = 255 \text{ nm}$. Under these conditions, the nonlinear absorption coefficient was obtained to be $-1.02 \times 10^{-6} \text{ cm W}^{-1}$, which was about one order of magnitude larger than azobenzene side-chain polymer reported before.¹⁷ As the shape of the Z-scan results for the substrates was flat, the nonlinear optical effect of the substrate can be neglected. The large optical nonlinearity mainly resulted from the polymer film.

From the CA Z-scan curve, the difference between normalized peak and valley transmittance ΔT_{p-v} can be directly measured. The variation of this quantity as a function of $|\Delta\phi_0|$ is given by Sheik-Bahae et al.¹⁴

$$\Delta T_{p-v} = 0.406(1 - S)^{0.25} |\Delta\phi_0|, \quad (4)$$

Here, $|\Delta\phi_0|$ is the on-axis phase shift at the focus, and it can be obtained from equation

$$|\Delta\phi_0| = kL_{\text{eff}} n_2 I_0 = (2\pi/\lambda) L_{\text{eff}} n_2 I_0, \quad (5)$$

where I_0 is the intensity of the laser beam at focus $z = 0$. S is the aperture linear transmittance. The peak followed by a valley-normalized transmittance obtained from the CA/OA curve in Figure 2 indicates that the sign of the nonlinear refraction is negative, which results from self-defocusing. The distance between the peak and valley is about 8.1 mm as compared to $1.7z_0$, which indicates that the nonlinear effect is a third-order nonlinear response. The nonlinear refractive index n_2 of the film is given according to the following equation:

$$n_2 = \frac{\Delta T_{p-v} \lambda}{0.406(1 - S)^{0.25} 2\pi L_{\text{eff}} I_0}. \quad (6)$$

The value of ΔT_{p-v} can be obtained to be 0.51 through the best theoretical fit from the result of the CA/OA Z-scan curve,

and the calculated value of n_2 is $-7.3 \times 10^{-11} \text{ cm}^2 \text{ W}^{-1}$, which is much larger than that of many other organic materials reported before.¹⁷⁻¹⁹

The real part and imaginary part of the nonlinear optical susceptibility could be evaluated from the nonlinear refractive index n_2 and nonlinear absorption coefficient β , respectively. The relations are defined as follows²⁰:

$$\begin{aligned} \text{Re}\chi^{(3)}(\text{esu}) &= (cn_0^2/120\pi^2)n_2(\text{m}^2/\text{W}) \text{ and} \\ \text{Im}\chi^{(3)}(\text{esu}) &= (c^2n_0^2/240\omega\pi^2)\beta(\text{m/W}), \end{aligned} \quad (7)$$

where c is the velocity of the light in vacuum, n_0 is the linear refractive index of the sample, and $\omega = 2\pi c/\lambda$ is the angular frequency of the light field. Thus, $\text{Re}\chi^{(3)}$ and $\text{Im}\chi^{(3)}$ were calculated as $4.16 \times 10^{-9} \text{ esu}$ and $2.53 \times 10^{-10} \text{ esu}$, respectively. The absolute value of $\chi^{(3)}$ was calculated from $|\chi^{(3)}(\text{esu})| = [(\text{Re}\chi^{(3)}(\text{esu}))^2 + (\text{Im}\chi^{(3)}(\text{esu}))^2]^{1/2}$ and gave $4.17 \times 10^{-9} \text{ esu}$.

The third-order nonlinearity observed is not induced by thermal effect within the pulse temporal width. Refractive index changes due to thermal nonlinearities arise from density changes in the materials propagating with acoustic wave speed caused by heating. If we estimate the acoustic wave speed to be on the order of $3 \times 10^3 \text{ m s}^{-1}$, the time to propagate a distance equal to the beam radius at focus is about 10 ns at 532 nm excitation, about 260 times longer than the pulse width. Obviously, thermal effects are, therefore, not expected to be important in experiments with picosecond duration laser. Also, in our experiment, the laser repetition rate is so low (10 Hz) that the cumulative thermal effects are negligible. It is most likely that the nonlinearity under ps 532 nm excitation is closely related to the S_0 to S_1 transition and the subsequent trans to cis transformation of the molecules. The photoinduced trans to cis transformation can occur within a subpicosecond timescale; it certainly takes place within the 38 ps pulse duration used in our experiment.¹³

The nonlinear optical response of the polymer film in femtosecond time scales was determined using OKE technique. A typical temporal behavior of the optical Kerr signal observed for the polymer film is shown in Figure 3. The OKE signal is nearly symmetric with a valley centered at zero delay point, and the full width at the half maximum of the Kerr signal is as fast as 300 fs, indicating that the optical response of the sample is very fast. In the OKE experiment, CS_2 is used as the reference. The $\chi^{(3)}$ of CS_2 is accredited as $0.67 \times 10^{-13} \text{ esu}$ in fs domain.²¹ Based on the magnitudes of the OKE signal of the sample and the reference under identical experimental condition, the $\chi^{(3)}$ of the polymer film is calculated as $6.8 \times 10^{-14} \text{ esu}$ according to the following formula²²:

$$\begin{aligned} \chi^{(3)} &= \chi_r^{(3)} \times \left(\frac{I_s}{I_r}\right)^{1/2} \times \left(\frac{n_s}{n_r}\right)^2 \times \left(\frac{L_r}{L_s}\right) \\ &\quad \times \frac{\alpha L_s}{\exp(-\frac{\alpha L_s}{2}) \times [1 - \exp(-\alpha L_s)]} \end{aligned} \quad (8)$$

where I is the intensity of the OKE signal at zero delay time, α is the linear absorption coefficient of the sample, n is the refractive index, and L is the interaction length of pump beam and probe beam over the CS_2 and the sample. The subscripts s and r denote

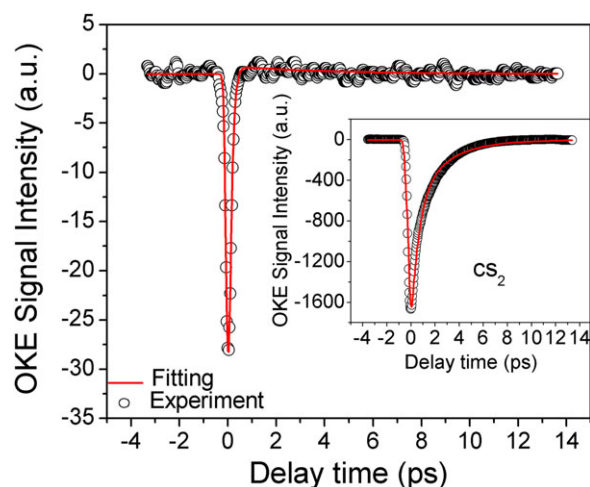


Figure 3. Time-resolved optical Kerr response of the polymer film. The inset is the OKE signal of CS₂ measured under the same conditions. The solid curve is the theoretical fit. [Color figure can be viewed in the online issue, which is available at wileyonlinelibrary.com.]

the sample and CS₂, respectively. As the excitation wavelength is far from any absorption resonance of the polymer, the ultrafast OKE response mainly arises from nonresonant electronic nonlinearity.

It is well known that the *trans*–*cis*–*trans* isomerization and reorientation of azobenzene group occur upon actinic irradiation. Furthermore, the in-plane orientation order of azo groups increases with laser fluences.^{23,24} Typical behaviors of photoinduced dichroism are presented in Figure 4. Before irradiation, the same absorption in any polarization direction indicated that no dichroism was obtained. However, the film exposed to the P-polarized irradiation over 20 min showed obvious dichroism. A strong difference in the polarized absorbance components was induced by the irradiation. The absorbance in the direction perpendicular to laser polarization was larger than the

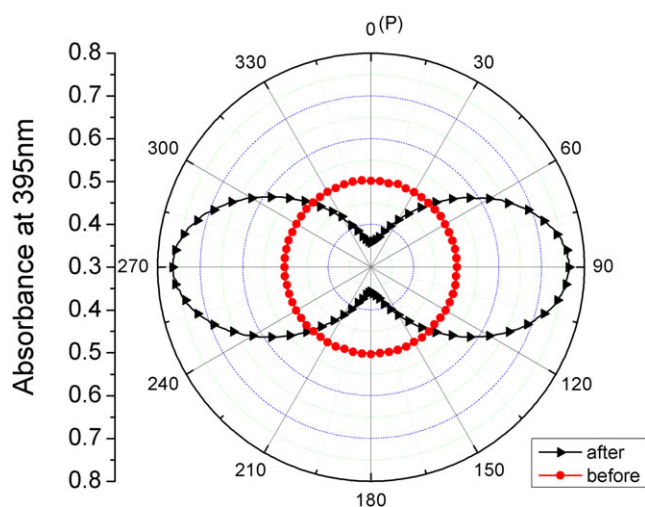


Figure 4. Polar plot of polarized absorbance before and after irradiation with polarized 405 nm laser (15 mW cm⁻²) over 20 min. [Color figure can be viewed in the online issue, which is available at wileyonlinelibrary.com.]

absorbance parallel to laser polarization, indicating that a significant number of azobenzene moieties have been aligned in the direction perpendicular to the pump polarization even though the pump intensity was 20 mW cm⁻². Stable value of the in-plane order parameter of 0.37 has been achieved in this material at room temperature. Figure 5 shows the polarized optical microscope (POM) image of the film after being irradiated for 20 min. The light field of the irradiated area presented alternative change of dark or bright under crossed polarizers according to the rotation of the sample with a period 90°, while it is always dark-field for the unirradiated area, indicating that the molecular alignment changed from disordered to ordered after irradiation.²⁵

To get a deeper understanding of the photoinduced anisotropy, the real-time behavior of photoinduced birefringence was investigated. Figure 6 shows the typical growth and relaxation of photoinduced birefringence at various pump intensities. The moments of turning on and off writing light are marked with arrows. When the pump is on, the signal of photoinduced birefringence reached 50% saturation in about 50 s and 90% in about 150 s in the writing process for the light intensity of 130 mW cm⁻². As the pump intensity increases, the saturation value of the birefringence reaches a maximum during the irradiation period. When the writing beam was switched off, the signal obviously increased until a stable value was reached. The large value of photoinduced birefringence ($\Delta n \sim 10^{-1}$) in the polymer film indicates that the material has potential value in the application of optical storage and LC display. The birefringence of this polymer film is several times larger than that reported in Ref. 26.

The observed inverse relaxation of the birefringence can be attributed to the cooperative interaction between mesogens, which was a character of the liquid crystalline polymer. The

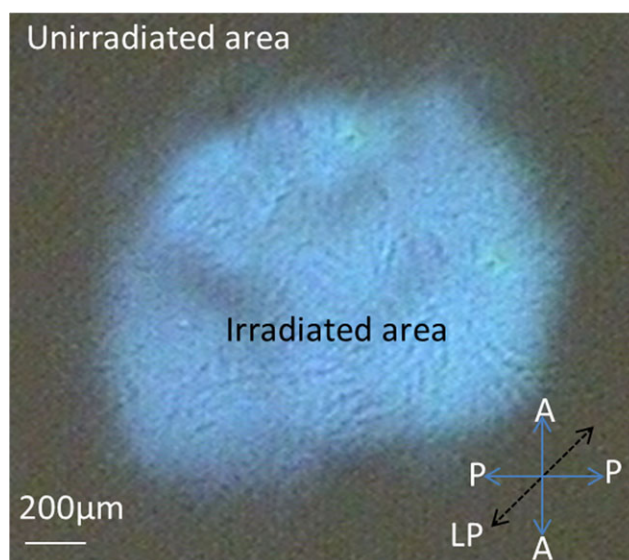


Figure 5. POM observed image of the polymer film upon linear polarized light irradiation. PP: the polarization direction of POM polarizer; AA: the polarization direction of POM analyzer; LP: the polarization direction of polarized pump light. [Color figure can be viewed in the online issue, which is available at wileyonlinelibrary.com.]

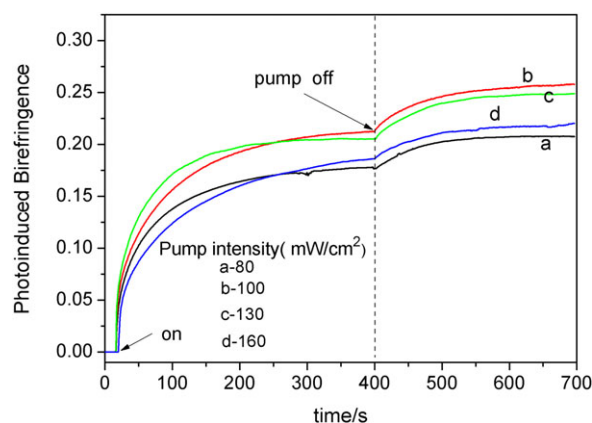


Figure 6. The signals of photoinduced birefringence for the azobenzene-containing polymer film at room temperature under various pump intensities: (a) 80 mW cm^{-2} , (b) 100 mW cm^{-2} , (c) 130 mW cm^{-2} , and (d) 160 mW cm^{-2} . [Color figure can be viewed in the online issue, which is available at wileyonlinelibrary.com.]

molecules which have not been reoriented aligned spontaneously along the direction of the molecules that have already been photo-aligned. The orientation existed in the initial film was the driving force for a further collective reorientation of the nonaligned molecules, resulting in an enhancement of birefringence. Several groups have reported the thermally amplification of the photoinduced birefringence of azobenzene-containing LC polymer.^{10,27} Since large magnitude of the anisotropy is strongly required to improve the optical performance and the stability of birefringence is often judged by the proportion of remnant birefringence after relaxation, the self-amplification of birefringence without thermal treatment is the most attractive property for liquid crystalline aligning materials. Furthermore, it was found that the amplified degree during the relaxation process was closely related to pumping fluences, and further research about the relaxation mechanism is under process now.

CONCLUSIONS

We have investigated the optical nonlinearity and photoinduced anisotropy of an azobenzene-containing ionic liquid crystalline polymer film. Z-scan measurements showed that the film exhibited large nonlinear refractive index under 38 ps pulse excitation. The ultrafast nonlinear optical response was determined using OKE technique at 800 nm, and the response time was as fast as 300 fs. Large photoinduced dichroism ($D \sim 0.37$) and photoinduced birefringence ($\Delta n \sim 10^{-1}$) were achieved in the polymer film. The birefringence remained unchanged in a dark room for more than 1 month and could be rewritten with no fatigue after erasure. The large and ultrafast response optical nonlinearity and remarkable photoinduced anisotropy of the polymer film indicate that it will have potential value in the application of nonlinear optical device and optical storage.

ACKNOWLEDGMENTS

This work was supported by the National Natural Science Foundation of China (No. 11174203) and the fund of State Key Laboratory on Fiber Optic Local Area Communication Networks.

REFERENCES

- Fuh, A. Y. G.; Lin, H. C.; Mo, T. S.; Chen, C. H. *Opt. Express* **2005**, *13*, 10634.
- He, T. C.; Wang, C. S.; Pan, X.; Wang, Y. L. *Phys. Lett. A* **2009**, *373*, 592.
- Lee, M. R.; Wang, J. R.; Lee, C. R.; Fuh, A. Y. G. *Appl. Phys. Lett.* **2004**, *85*, 5822.
- Pan, X.; Wang, C. S.; Wang, C. Y.; Zhang, X. Q. *Appl. Opt.* **2007**, *47*, 93.
- Nedelchev, L. L.; Matharu, A. S.; Hvilsted, S.; Ramanujam, P. S. *Appl. Opt.* **2003**, *42*, 5918.
- Cui, L.; Zhao, Y. *Chem. Mater.* **2004**, *16*, 2076.
- Ono, H.; Emoto, A.; Takahashi, F.; Kawatsuki, N.; Hasegawa, T. J. *Appl. Phys.* **2003**, *94*, 1298.
- Uchida, E.; Kawatsuki, N. *Polymer* **2006**, *47*, 2322.
- Zakrevskyy, Y.; Stumpe, J.; Faul, C. F. J. *Adv. Mater.* **2006**, *18*, 2133.
- Hernandez-Ainsa, S.; Alcala, R.; Barbera, J.; Marcos, M.; Sanchez, C.; Serrano, J. L. *Macromolecules* **2010**, *43*, 2660.
- Zakrevskyy, Y.; Stumpe, J.; Smarsly, B.; Faul, C. F. J. *Phys. Rev. E* **2007**, *75*, 031703.
- He, T. C.; Wang, C. S.; Pan, X. *Physica B* **2008**, *403*, 2991.
- Rangle-Rojo, R.; Yamada, S.; Matsuda, H.; Yankelevich, D. *Appl. Phys. Lett.* **1998**, *72*, 1021.
- Sheik-Bahae, M.; Said, A. A.; Wei, T. H.; Hagan, D. J.; Stryland, E. W. V. *IEEE J. Quantum Electron.* **1990**, *26*, 760.
- Kawatsuki, N.; Yamashita, A.; Kondo, M.; Matsumoto, T.; Shioda, T.; Emoto, A.; Ono, H. *Polymer* **2010**, *51*, 2849.
- Todorov, T.; Nikolova, L.; Tomova, N. *Appl. Opt.* **1984**, *23*, 4309.
- He, T. C.; Cheng, Y. G.; Wang, C. S.; Jia, T. J.; Li, P. W.; Mo, Y. J. *Phys. Stat. Sol. (b)* **2007**, *244*, 2166–2171.
- He, T. C.; Wang, C. S.; Pan, X.; Zhang, C. Z.; and Lu, G. Y. *Appl. Phys. B* **2009**, *94*, 653.
- Cheng, P. H.; Zhu, H. L.; Bai, Y. K.; Zhang, Y.K; He, T. C.; Mo, Y. J. *Opt. Commun.* **2007**, *270*, 391.
- Yang, G.; Wang, H.H.; Tan, G. T.; Jiang, A. Q.; Zhou, Y. L.; Chen, Z. H. *Appl. Opt.* **2002**, *41*, 1729.
- Li, D.; Liu, Y.; Yang, H. Q.; Qian, S. X. *Appl. Phys. Lett.* **2002**, *81*, 2088.
- Imanishi, Y.; Ishihara, S. *Thin Solid Films* **1998**, *331*, 309.
- Li, X.; Lu, X. M.; Lu, Q. H.; Yan, D. Y. *Macromolecules* **2007**, *40*, 3306.
- Priimagi, A.; Vapaavuori, J.; Rodrigue, F. J.; Faul, C. F. J.; Heino, M. T.; Ikkala, O.; Kauranen, M.; Kaivola, M. *Chem. Mater.* **2008**, *20*, 6358.
- Xiao, S. F.; Lu, X. M.; Lu, Q. H. *Macromolecules* **2007**, *40*, 7944.
- Pan X.; Xiao S. F.; Wang, C. S.; Cai, P.; Lu, X. M.; Lu, Q. H. *Opt. Commun.* **2009**, *282*, 763.
- Minabe, J.; Kawano, K.; Nishikata, Y. *Appl. Opt.* **2002**, *41*, 700.